Article citation info:
SAWCZUK W. Analytical model coefficient of friction (COF) of rail disc brake on the basis of multi-phase stationary tests. Eksploatacja i Niezawodnosc – Maintenance and Reliability 2018; 20 (1): 57–67, http://dx.doi.org/10.17531/ein.2018.1.8.

Wojciech SAWCZUK

ANALYTICAL MODEL COEFFICIENT OF FRICTION (COF) OF RAIL DISC BRAKE ON THE BASIS OF MULTI-PHASE STATIONARY TESTS

MODEL ANALITYCZNY ZMIENNOŚCI WSPÓŁCZYNNIKA TARCIA KOLEJOWEGO HAMULCA TARCZOWEGO NA PODSTAWIE WIELOFAZOWYCH BADAŃ STANOWISKOWYCH*

Similarly to road vehicles, a disc brake remains the main friction brake in rail vehicles. Due to the increasing train speeds, a disc brake has already replaced the traditional clasp brake that is however, still used in cargo trains. In the process of long-term operation of the brake pad-brake disc friction pair, the parameters of the braking process such as the curve of the coefficient of friction are changed, which extends the braking distance. The paper presents the results of several years of investigations on the railway disc brake in different wear conditions in the aspect of the requirements set by the UIC (International Union of Railways) related to the brake pads approval for use.

***Keywords**: railway disc brake, organic brake pad, coefficient of friction, multiple regression.*

W pojazdach szynowych, podobnie jak w samochodowych, podstawowym hamulcem roboczym jest cierny hamulec tarczowy. Ze względu na coraz większe prędkości jazdy, hamulec tarczowy w wielu pojazdach kolejowych jak i tramwajowych wyparł już hamulec klockowy, który niezmiennie jeszcze jest stosowany w pociągach towarowych. W procesie dłuższej eksploatacji pary ciernej tarcza-okładzina główne parametry procesu hamowania jak przebieg współczynnika tarcia obniża się, co w konsekwencji wydłuża drogę hamowania. W artykule przedstawiono wyniki kilkuletnich badań kolejowego hamulca tarczowego w różnych stanach jego zużycia z uwzględnieniem między innymi wymagań stawianych przez Międzynarodowy Związek Kolei UIC w zakresie dopuszczenia okładzin hamulcowych do eksploatacji.

***Słowa kluczowe**: kolejowy hamulec tarczowy, współczynnik tarcia, regresja wieloraka.*

1. Introduction

Due to the nature of friction in the disc brake (dry friction), it is possible to apply this brake to different friction models. In case of vehicle standstill, it is possible to refer to static friction models such as Karnopp [21], Quinn, Awrejcewicz [4, 12], Adams [8] or Wojewody [55]. These models are based on the Coulomb model. However, dynamic braking models (derived from the Dahl model) such as the LuGre model [34, 40], the Leuven model [30] and the GMS model [2] are used during the braking process from set speed to stop. The operating range of the disc brake is very complex in terms of speed or load as well as the state of the transition between the friction and the kinetic friction. A large number of variable parameters hinder the process of friction modeling in the brake system, resulting in significant model development and longer computational time.

The friction pair of a railway disc brake must meet a variety of regulatory requirements before it is approved for use. TSI (Technical Inter-operation Specifications) regulations related to the UIC sheets are applicable for the brake pads and for the brake discs PN-EN standards apply. This is sometimes validated with several days of testing on test stands. In order to most efficiently reproduce the conditions of a train braking with a disc brake, the tests are carried out in the 1:1 scale on actual objects. Due to the size of the test stand and the costs of its maintenance there are only a few such tests stands in Europe, contrary to the tests stands designed for road vehicles (most often owned by brake pad manufacturers). The friction pads of the disc brake are made of an organic material consisting of thermo hardened resins, synthetic elastomers, friction modifiers and metallic fibers [25, 52]. The second typical friction pad material is metallic sintered composites containing a number of matrix and non-metal metallic components in the form of sliding, friction and filler additives [23, 25]. In the case of motor vehicles, there are also ceramic friction pads [38, 39, 54] characterized by a more stable friction coefficient compared to the composite material.

Validation tests on test stands are preceded by laboratory tests on the friction material samples and simulations in the ANSYS or ABAQUS environment [6, 22, 36]. Tests provide the possibility of evaluation of the temperature distribution on the brake disc as presented in [9, 20, 42]. In terms of temperature distribution, many researchers deal with the problems of explanation and modeling of the phenomenon of hot spots occurring on the surface of the brake discs or vehicle clutches, as discussed in [23, 29]. A separate problem raised by many researchers [19, 23, 49, 57] is the process of fatigue cracking of brake discs by cyclical heating during braking and cooling of the disc after braking (disc spectrum). As a result of the rapid increase of the disk temperature and its equally rapid (in the case of ventilated discs) or slow (for full discs) cooling, there are surface cracks occurring on the surface of friction disc in the form of microcrystalline grids. Figure 1 shows the typical damage to the brake discs in terms of single cracks on the friction surface and microcracks on a substantial portion of the disc surface.

The phenomenon of thermal cracking is identifiable only after a series of brakings (approx. 300 and more) on the test stand or during operation (heavy-duty trucks in particular). A separate phenomenon occurring in the operation of the disc brake is the uneven wear of the

(*) Tekst artykułu w polskiej wersji językowej dostępny w elektronicznym wydaniu kwartalnika na stronie ***www.ein.org.pl***

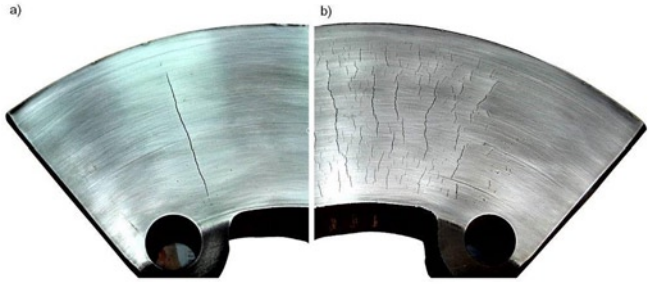

Fig. 1. View of friction disc brake discs after several years of use: a) with one crack, b) with surface cracks

friction pads due to the poor alignment of the pads relative to the disc. In the paper [19] the results of friction brake discs wear from the operation of double-deck passenger rail cars type Bmnopux. The work presents examples of uneven wear of friction linings such as higher wear on the outer radius of the disc relative to the inner radius of the disc, edge defects and cracking or tearing of the entire lining parts from the bearing plate. In this respect, works are underway on such a selection of the friction pair materials as to ensure a compromise among the costs of manufacturing (additional thermal and chemical processes when making the casts of the brake discs), the component wear and the friction mechanical properties of the friction pair, as described in [1, 3, 10, 13, 14, 42]. On the other hand, [7, 11, 37] presents problems related to friction models and friction wear modeling of brake system components based on operational tests. A separate issue raised by many researchers in [24, 31, 52] is the vibration and noise generated by brakes during braking. In papers [17, 18, 50, 51], vibroacoustic signals in the time domain, amplitudes and frequencies have been analyzed, allowing for the evaluation of rotary machines, brakes and identification of faults.

The aim of this article is to present a model for estimating the mean friction coefficient of the disc brake in terms of braking parameters as well as some parameters of the design and operation of the friction pair of disc brake discs. Modeling of the coefficient of friction using multiple regression was carried out on the basis of several years of examination of the rail brake disk at the brake position in terms of both momentary and average friction coefficient. It should be emphasized that the current provisions for the admission of such brake system components as brake disc and friction lining are reduced to a positive test result at a certified brake position only for new (unused) brake discs and lining without frictional characteristics for parts or completely worn out.

2. Requirements set for the disc brake friction pair

In railway vehicles, two types of brake linings are applied made from either organic or sintered materials, as shown in Fig. 2.

Depending on the applied brake lining, during tests on approved test stands, appropriate characteristics of the curve of instantaneous and average coefficient of friction are developed.

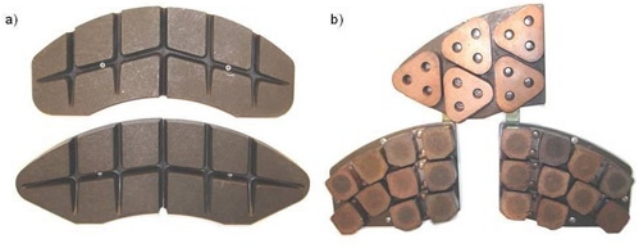

Fig. 2. View of the brake pads used in a railway disc brake: a) organic material, b) sintered material

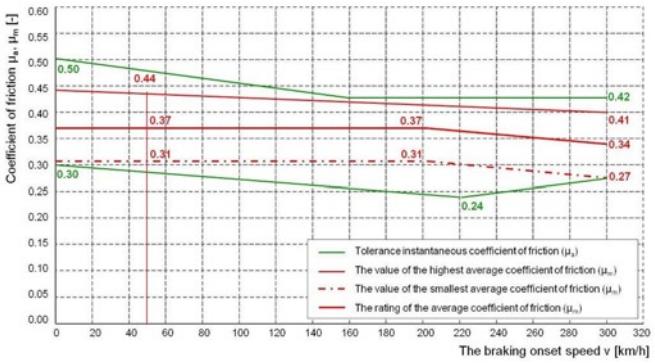

Fig. 3. Range of tolerance of the coefficients of friction of a friction pair of a railway disc brake during the tests on the test stand according to [26]

A brake lining made from an organic and sintered material according to [26] must ensure a curve of the coefficient of friction of a friction pair in a dry condition on the level of 0.37. The tolerance ranges of the instantaneous and average coefficients of friction have been shown in Fig. 3. Besides, the main requirement for the railway brake linings according to UIC 541-3 is an absolute restriction on the application of blue asbestos. UIC 541-3 does not recommend the use of lead, zinc and other materials whose dust or gas generated during braking may have an adverse effect on the passengers and be hazardous to their health.

The brake lining material should be selected to ensure a balance between:

- friction properties of the friction pair,
- wear and durability of the brake pads,
- negative impact on the brake disc.
- Besides, the coefficient of friction of the friction pair in a disc brake should possibly be independent from:
- braking onset speeds,
- clamping force of the brake pads on the brake disc,
- the run-in condition of the brake pads,
- atmospheric conditions (rain, snow),
- temperature of the surface of the disc brake.

Under the influence of humidity, snow or ice a slight deviation of the average coefficient of friction is allowed compared to braking performed under dry conditions. The average coefficient of friction under these conditions may vary in relation to the braking performed under dry conditions in the range of ± 15%. The average coefficient of friction of a friction pair when braking under dry conditions until a full halt performed at the temperature of the friction surface of above 140°C may be different than a braking performed on a cold disc (max. 60°C) not more than 15% [26].

During continuous braking (simulation of a coast down) with the maximum power of up to 43 kW per friction pair, the coefficient of friction should meet the following requirements [26]:

- The average coefficient of friction from the entire braking process should fall between 0.25 and 0.50,
- The amplitude of the course of instantaneous coefficient of friction should not exceed 0.15.

The above requirements should be met by the organic friction material up to 400°C (the disc temperature) and 550°C when the brake linings are made from metallic sinters [26].

Besides, the TSI regulations and sheets [26, 27, 47, 48], related to the requirements for brake linings of a discs brake, state that the friction material must meet requirements related to the tolerance of instantaneous and average coefficient of friction in the entire range of admissible brake pad wear level, i.e. 5 mm from the 35 mm thickness of a new pad.

For brake discs complying to the [43, 45] standards, depending on the program of research, the requirements pertain to the dissipated en-

ergy, braking power, braking onset speeds, decelerated mass per single brake disc and brake delay. Depending on the program of research simulating the braking of a light railcar or, in an extreme scenario, a locomotive or a traction set from high speeds, the required energy to be dissipated falls in the range of 4.6÷37 MJ. The braking powers during braking should fall in the range 400÷667 kW at the braking onset speeds falling in the range of 120÷400 km/h. During the stationary investigations, the decelerated masses are 6÷10 t depending on the type of braking, while the braking delays during the investigations should not exceed 0.8÷1.2 m/s^2. In the most recent editions of standard [45] more requirements were introduced related to the energy absorbed by the ventilated brake discs when disengaged and rotating (simulation of a train drive at a steady speed without braking) and the noise generated by the disc brake during the tests. Depending on the applied ventilated brake disc, the power used during its rotation should not exceed 5kW. Schedule B to standard [45] contains the methodology of the noise measurement without not-to-exceed boundary values related to the disc brake during braking. In regulation 90 [53] related to the brake discs (despite the fact that this pertains to road vehicles) additional requirements are included as to the content of carbon, silicon, manganese, chromium and copper, depending on the disc type (cast iron, cast steel, carbon or alloy). Besides, the regulation states the ranges of hardness (for cast iron discs 190÷248 HBW) and geometrical quantities of the discs to be met after mechanical processing (change of thickness, axial run out, surface perpendicularity, flatness and roughness). For railway brake discs, the geometrical quantities are provided only in the Operation and Maintenance Manual of a given vehicle (locomotive, traction set or railcar).

3. Methodology and object of investigations

Investigations related to the determination of selected braking characteristics depending on the conditions of the disc brake friction pair were performed based on the assumptions of an active experiment [32, 35]. During the tests, the input parameters (brake condition) were purposefully modified in a predefined way and their influence on the change of the output parameters was observed.

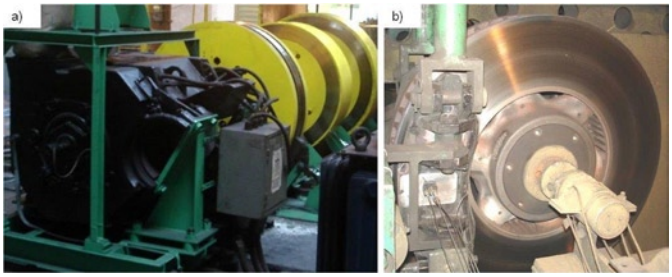

Fig. 4. View of the research object on the test stand: a) view of the driving section of the test stand with the rotating masses, b) 610×110 brake disc fitted on the test stand

Investigations of a tribological nature were performed on an inertia test stand presented in Fig. 4. On the said test stand, clasp brakes and disc brakes can be tested reproducing the rail vehicle actual braking conditions.

Two ventilated 610×110 gray cast iron brake discs were tested. The first disc was new and the other was worn to 105 mm from 110 mm (prior to tests). The worn disc was subject to turning. The brake disc masses were m_{T1}=116.0 kg (new disc) and m_{T2}=111.5 kg (disc worn). Both discs were prepared for the tests as per standard [44]. Fig. 5 presents the brake discs during the tests. In the tests, organic brake linings were applied.

The brake pads, according to the manufacturer's procedure and requirements contained in [26], were made from thermo bonded resin, synthetic elastomer, metal and organic fiber as well as friction modifiers. Three sets of brake pads were used per disc for the tests stand investigations (the first, new set of brake pads (4 pieces) - G_1=35 mm and the two sets of pads worn to G_2=25 mm and G_3=15 mm). Masses of friction pads were m_{G1}=1.75 kg (new pad), m_{G2}=1.45 kg (pad worn to 25 mm thickness), m_{G3}=1.02 kg (pad worn to 15 mm thickness). The applied brake pads have been shown in Figure 6.

Fig. 5. View of the brake discs used during the tests: a) disc worn to 104 mm after tests on the test stand, b) new disc of the thickness of 110 mm

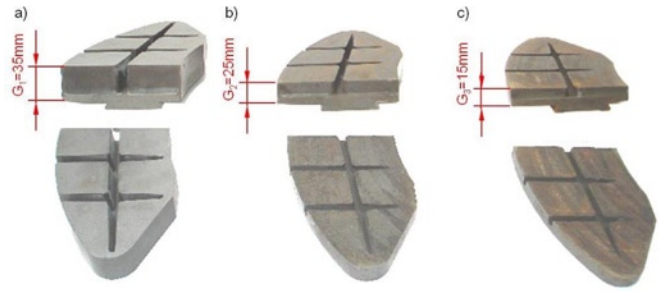

Fig. 6. View of the brake pads used during the tests: a) new brake pads, 35 mm, b) pads worn to 25 mm, c) pads worn to 15 mm

The tests stand investigations have been performed according to the UIC 541-3 sheet. Each research program refers to specific conditions of the brake operation throughout the vehicle life cycle. In order to reproduce the actual braking conditions with a disc brake of a passenger railcar, research program *C* has been selected – fast driving.

The modified parameters during the tribological tests were:
- conditions of the brake disc: new – 110 mm and worn – 105 mm,
- thickness of the brake pad: G_1=35 mm, G_2=25 mm and G_3=15 mm,
- Braking onset speed: v= 50, 80, 120, 160 and 200 km/h,
- clamping force of the pad on the disc: p= 28 and 44 kN,
- Decelerated mass per disc: M= 4.4 and 7.5 t.

Prior to the commencement of the main tribological investigations a series of brakings was performed to run in the brake pads. According to [26] initial braking needs to be continued until the surface is refreshed (exceeding 75% of the surface before running in.)

During the investigations on the inertia test stand, instantaneous coefficient of friction μ_a was recorded at each moment of braking [52]:

$$\mu_a = \frac{F_t}{F_b} \quad (1)$$

where: F_t – instantaneous tangential force related to the braking radius r,
F_b – total instantaneous clamping force on the brake disc.

Then, the average coefficient of friction μ_m was calculated determined from the definite integral of the instantaneous coefficient of friction throughout the braking distance s_2 [26]:

$$\mu_m = \frac{1}{s_2}\int_0^{s_2} \mu_a ds \quad (2)$$

Prior to the tests stand tribological investigations (upon running in of the brake pads), a series of 30 brakings were performed for statistical evaluation. The test aimed at determining of the minimum number of repetitions that would ensure the results on a satisfactory level of confidence of 95% at the adopted level of significance of α=0.05, at which the smallest coefficient of variation is observed. The value of the average slide coefficient of friction μ_m was subjected to analysis measured in 30 trials at an unchanged braking onset speed of 120 km/h. The measurement was performed upon running in of the brake pads according to the requirements contained in the UIC 541-3 sheet. Each subsequent braking was preceded by chilling of the disc through its free rotation, which also simulated the train driving at the speed of 100 km/h. Upon reducing of the disc temperature to 60°C, the chilling was stopped and subsequent braking was performed. In order to determine the minimum number of brakings, relations of the following statistical formulas were used: average value, standard deviation, half interval of confidence, bottom and top limit of the confidence interval and the coefficient of variation W based on [16, 28].

Fig. 7 presents the value of the coefficient of friction obtained from a given braking and the average value of the coefficient of friction taking into account the top and the bottom limits of the confidence interval with the assumed significance level of α=0.05 for two tested brake discs.

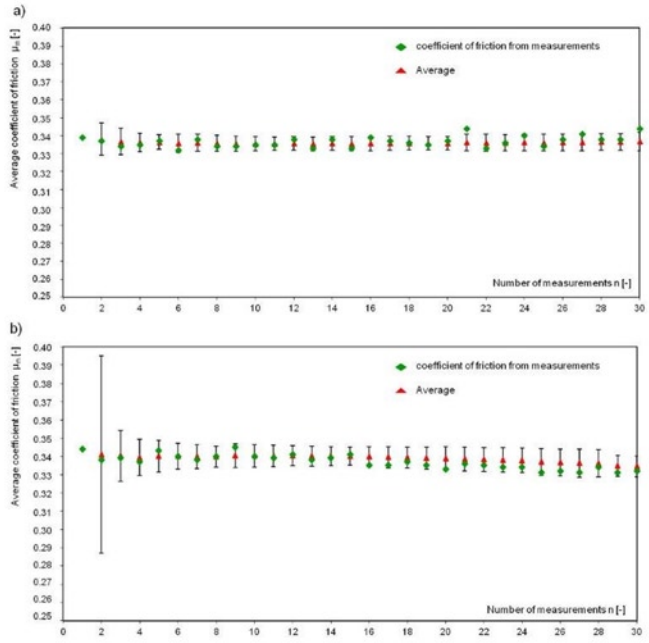

Fig. 7. Curve of the coefficient of friction between the brake pad and the brake disc and its average value obtained on the 610×110 disc: a) new, b) worn (turned)

Fig. 8 presents the percentage curve of coefficient of variation W determined in the measurement of the coefficient of friction, based on which the determination of the number of measurements was possible. Based on Fig. 7, upon performance of 30 brakings, it was observed that the minimum number of braking repetitions ensuring the obtainment of the average coefficient of friction in the expected confidence interval at the assumed level of significance of α=0.05, is 5 for the new disc and 8 for the worn one (turned).

Based on the statistical analysis of the obtained results of the measurement of the average coefficient of friction, disc temperature, braking distance and time, it was assumed that for the main investigations on the test stand 8 repetitions must be performed. For this number of brakings, a satisfactory coefficient of variance was obtained in the expected confidence interval and at the assumed level of significance. Since the values of the coefficient of variation for the measurements of the average coefficient of friction according to [16] did not exceed 10%, a negligible statistical difference of the analyzed quantities was observed.

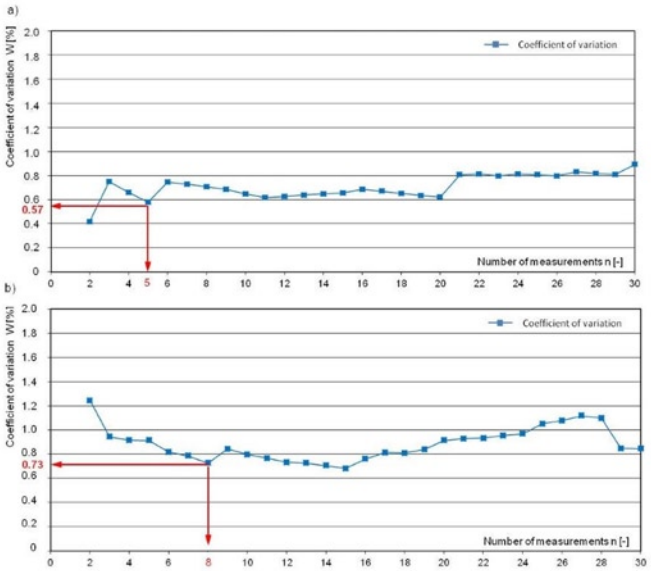

Fig. 8. Curve of the coefficient of variation obtained from the statistical calculations for the brake disc: a) new, b) worn (turned)

During tribological research, 780 brake applications were performed, not counting the brakes related to the lining of the friction lining. In order to validate the multiple regression model described by the relation (3) and presented in Chapter 5, further 384 inhibition was performed.

4. Results and analysis

The aim of the test stand investigations was to determine the curves of instantaneous and average coefficients of friction as per relations (1) and (2) with reference to the applicable regulations on the approval of brake pads of a disc brake for use.

The results of the investigations of the instantaneous coefficient of friction for three brake pads (35, 25 and 15 mm) and two brake discs have been presented in Figs. 9-12 allowing for the top and the bottom limits of the instantaneous coefficient of friction for rail vehicles in compliance with sheet [26]. By using relation (2), upon integrating of the value of instantaneous coefficient of friction on braking distance s, the average value of the coefficient of friction was obtained. The relations of the average coefficient of friction for the same braking parameters as in the instantaneous coefficient of friction have been shown in Figs. 13-16 The results have been referred to the top and

the bottom deviation of the average coefficient of friction, which also remained in compliance with sheet [26].

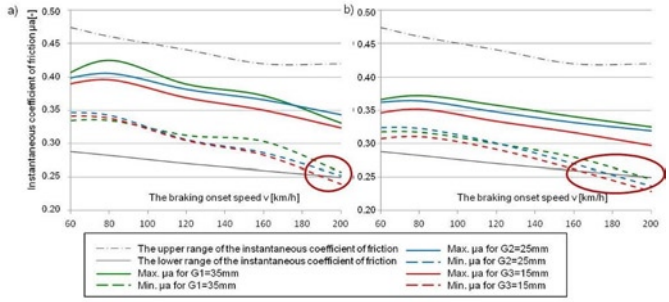

Fig. 9. Dependence of instantaneous coefficient of friction μ_a on the braking onset speed at N=44 kN, M=7.5 t: a) for a new disc, b) for a worn disc

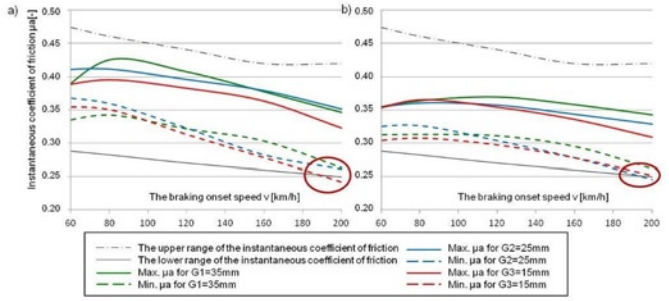

Fig. 10. Dependence of instantaneous coefficient of friction μ_a on the braking onset speed at N=28 kN, M=7.5 t: a) for a new disc, b) for a worn disc

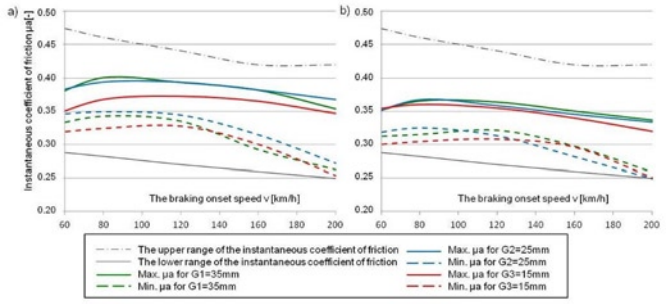

Fig. 11. Dependence of instantaneous coefficient of friction μ_a on the braking onset speed at N=44 kN, M=4.4 t: a) for a new disc, b) for a worn disc

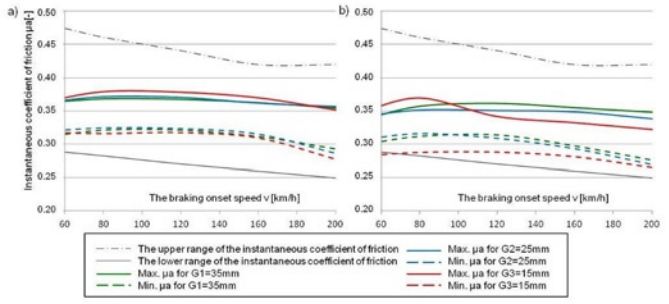

Fig. 12. Dependence of instantaneous coefficient of friction μ_a on the braking onset speed at N=28 kN, M=4.4 t: a) for a new disc, b) for a worn disc

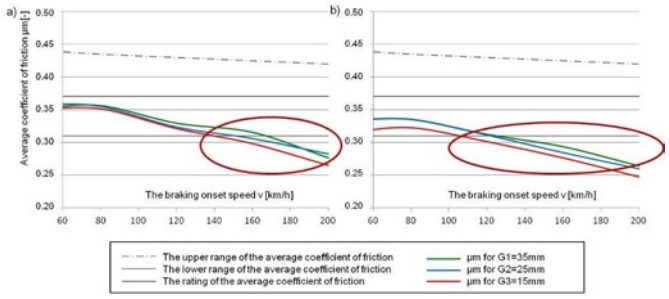

Fig. 13. Dependence of average coefficient of friction μ_m on the braking onset speed at N=44 kN, M=7.5 t: a) for a new disc, b) for a worn disc

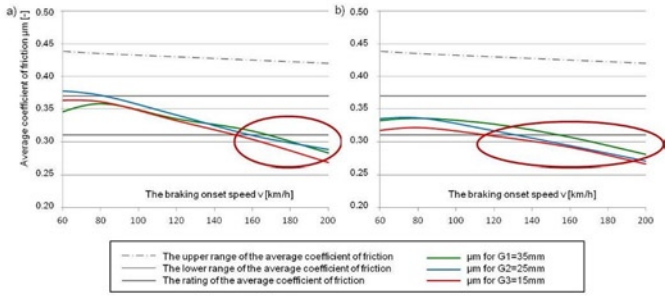

Fig. 14. Dependence of average coefficient of friction μ_m on the braking onset speed at N=28 kN, M=7.5 t: a) for a new disc, b) for a worn disc

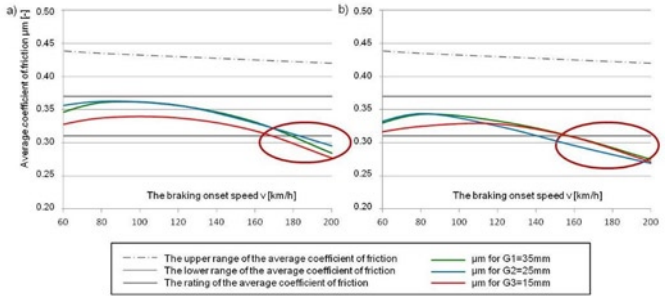

Fig. 15. Dependence of average coefficient of friction μ_m on the braking onset speed at N=44 kN, M=4.4 t: a) for a new disc, b) for a worn disc

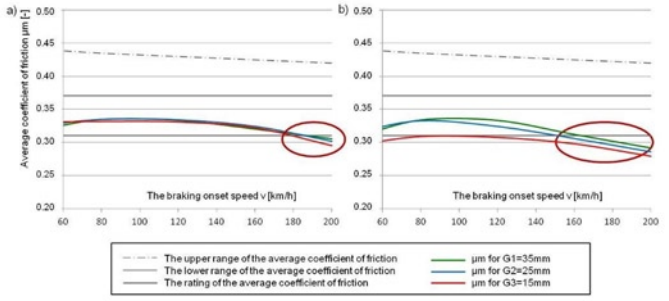

Fig. 16. Dependence of average coefficient of friction μ_m on the braking onset speed at N=28 kN, M=4.4 t: a) for a new disc, b) for a worn disc

Upon analysis of the curves of the instantaneous coefficient of friction presented in Figs. 9-12 one can observe that in some combinations of the clamping force and decelerated mass, the obtained values of the minimum coefficient of friction exceed the minimum required range μ_a of instantaneous coefficient of friction according to sheet [26]. This is particularly the case for a disc worn to 105 mm cooperating with brake pads worn to 15 mm while braking with high

clamping force (N=44 kN) and decelerated mass of M=7.5 t simulating the braking process of a railcar with a maximum load at the speed of v=200 km/h. For the brakings performed on a new disc, only worn brake pads influence the instantaneous coefficient of friction at the bottom tolerance limit μ_a at the braking onset speed of 200 km/h. It is to be expected though, that at higher braking onset speeds (from 200 to 300 km/h), as provided in sheet UIC 541-3, the bottom limit of instantaneous coefficient of friction will be exceeded, as provided in the above sheet.

Upon analysis of the curves of average coefficient of friction obtained during the investigations, it can be observed that for all braking scenarios the bottom deviation of the average coefficient of friction is exceeded for both new and worn discs, for all brake pad configurations (new and worn). Only in the case of low clamping force braking and low decelerated mass (N=28 kN and M=4.4 t) on a new disc and new brake pads up to the braking onset speed of v=200 km/h was the non-excess of the average coefficient of friction above its bottom value observed. For the braking with a high value of the clamping force and a high decelerated mass (N=44 kN and M=7.5 t), the analyzed case of braking using a new disc and worn brake pads results in a non-compliance with the bottom limit of the average coefficient of friction starting from the braking onset speed of v=140 km/h and, in the case of a worn disc and worn pads, from the speed of v=100 km/h. It is noteworthy that in the investigations no extreme case of maximum admissible disc and brake pad wear was considered. Based on the Operation and Maintenance Manual [15, 46], it is allowed to use a brake disc worn to 102 mm (repetitive turning) and brake pads worn to 5 mm based on sheet [26]. In the tests the author used a disc of the thickness of 104 mm and brake pads worn to 15 mm.

5. Modeling of the variation of the coefficient of friction

Based on the results of the investigations of average coefficient of friction $\mu_{m,}$ modeling of its variation was attempted based on such input parameters as disc thickness, brake pad thickness, braking onset speed, clamping force of the pad on the disc and decelerated mass per one disc.

Multiple regression (otherwise referred to as multinomial regression) was applied to model the variation of the average coefficient of friction. This is a method, in which the value of a random variable Y depends on k-th dependent attributes (X_1, X_2, ... X_k). Based on a given sample of the results, according to [16], determination of the invariable parameters α_0, α_1, ... α_k was performed using the method of least squares. The following relation was proposed to determine the coefficient of friction:

$$\mu_m = \alpha_1 G_T + \alpha_2 G_O + \alpha_3 v^2 + \alpha_4 v + \alpha_5 N + \alpha_6 M + \alpha_0 \qquad (3)$$

where: G_T – thickness of the brake disc (new 110 mm, worn to 105 mm),
G_O – thickness of the brake pads (new G_1=35 mm, worn to G_2=25 mm and G_3=15 mm),
v – braking onset speed (v=50, 80, 120, 160 and 200 km/h),
N – clamping force of the brake pad on the disc (N=28 and 44 kN),
M – decelerated mass per one disc (M=4.4 and 7.5 t).

Calculated multiple regression parameters for the model (3) obtained at the determinant R^2=0.81 are summarized in Table 1.

Then, the Pearson linear correlation coefficient was validated according to relation (4) for the analyzed variables i.e. disc thickness, thickness of the brake pads, braking onset speeds, clamping force of the brake pads on the disc and decelerated mass.

Table 1. Coefficient of multiple regression

Coefficient	Value
α_1	$3.72 \cdot 10^{-3}$
α_2	$5.09 \cdot 10^{-4}$
α_3	$-3.78 \cdot 10^{-6}$
α_4	$5.66 \cdot 10^{-4}$
α_5	$-4.92 \cdot 10^{-5}$
α_6	$-8.81 \cdot 10^{-4}$
α_0	$-90.2 \cdot 10^{-3}$

$$r = \frac{\sum_{i=1}^{n}\left(x_i - \bar{x}\right)\left(y_i - \bar{y}\right)}{\sqrt{\sum_{i=1}^{n}\left(x_i - \bar{x}\right)^2 \sum_{i=1}^{n}\left(y_i - \bar{y}\right)^2}} \qquad (4)$$

where:

$\bar{y}$, $\bar{x}$ – average values of attribute x and attribute y,
y_i, x_i – descriptive values.

Table 2 presents the correlation matrix (Pearson) for the analyzed variables. Upon analysis of the correlation coefficient from table 2 it was observed that the changes of the average coefficient of friction are most heavily influenced by the braking onset speeds (r=0.79) and the clamping force of the brake pads on the disc (r=0.0146) while the decelerated mass (R=0.0507) has the least influence. The model written with relation (3) may be simplified by eliminating the influence of two variables i.e. the clamping force and the decelerated mass.

Figs. 17-20 present the validation of the model of regression as per relation (3) against the results of investigations of the average coefficient of friction obtained on the test stand.

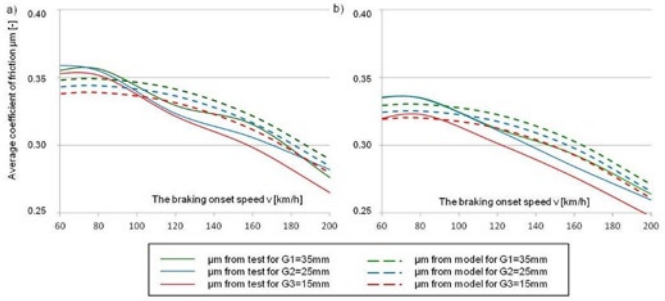

Fig. 17. The relation between the average coefficient of friction obtained in the tests and that allowing for the model of multiple regression when braking with N=44 kN, M=7.5 t: a) new disc, b) worn disc

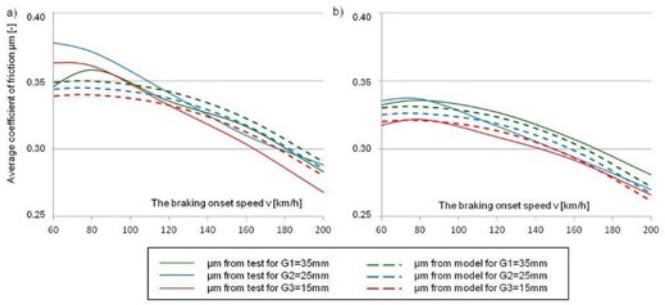

Fig. 18. The relation between the average coefficient of friction obtained in the tests and that allowing for the model of multiple regression when braking with N=28 kN, M=7.5 t: a) new disc, b) worn disc

Table 2. Correlation matrix

Variable	Disc sickness G_T	Brake pad thickness G_O	Speed v^2	Speed v	Brake pad clamping force N	Decelerated mass M	Correlation coefficient
Disc thickness G_T	1.0	0	0	0	0	0	0.3449
Brake pad thickness G_O	0	1.0	0	0	0	0	0.1542
Speed v^2	0	0	1.0	0.9855	0	0	−0.7998
Speed v	0	0	0.9855	1.0	0	0	−0.7557
Brake pad clamping force N	0	0	0	0	1.0	0	−0.0146
Decelerated mass M	0	0	0	0	0	1.0	−0.0507
Correlation coefficient	0.3449	0.1542	−0.7998	−0.7557	−0.0146	−0.0507	1.0

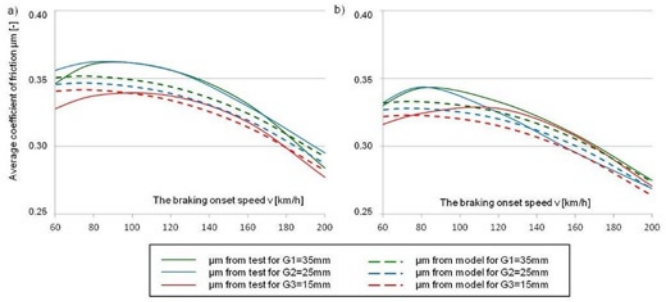

Fig. 19. The relation between the average coefficient of friction obtained in the tests and that allowing for the model of multiple regression when braking with N=44 kN, M=4.4 t: a) new disc, b) worn disc

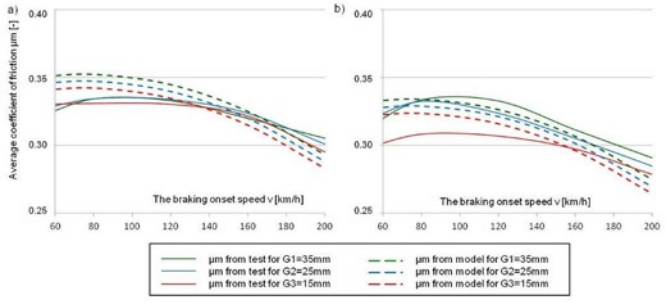

Fig. 20. The relation between the average coefficient of friction obtained in the tests and that allowing for the model of multiple regression when braking with N=28 kN, M=4.4 t: a) new disc, b) worn disc

Then, according to relation (5) the relative percentage error was determined [28] of the fitting of the model of multiple regression of the average coefficient of friction to the results of the investigations.

$$\delta = \frac{|x - x_z|}{x} \cdot 100\% \tag{5}$$

where: x – value μ_m obtained in the tests on the test stand,
x_z – value μ_m determined from the model of multiple regression (relation (3)).

Due to the sample size of $n>30$, based on inequality (6) a number of k classes was set in order to determine the distribution of the relative percentage error [16].

$$k \leq 5 \ln n \tag{6}$$

Upon the application of relation (6) the number of k classes was 10. Based on the relative error data, the maximum value of variable x_{max}=9.8 and the minimum value x_{min}=0.009 were determined, which allowed the calculation of the data spread of 9.79. Fig. 21 shows the histogram of the relative percentage error size for 10 classes.

Upon the analysis of the histogram presented in Fig. 21 it can be observed that the greatest is the relative error resulting

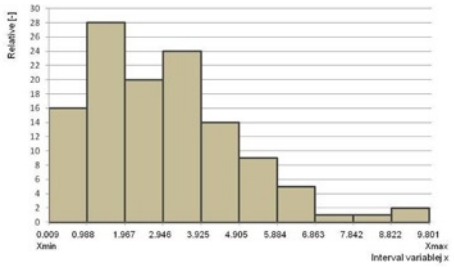

Fig. 21. Histogram of the relative percentage error size of the fitting of the model of average coefficient of friction to the results of the investigations

from the non-fitting of the model of multiple regression to the results in the range of up to 2% that occurred in 44 cases out of 120 observations. The error in the range of up to 5% occurred in 88 cases.

6. Model validation

In order to check the proposed model of estimation of the average coefficient of friction, a model validation was performed from equation (3) on subsequent brake discs. The tests were performed on two brake discs (new and regenerated) obtained from different suppliers and brake pads made from organic material. During the investigations, three types of brake pads were prepared (FR20H.2), one set of new brake pads (4 pieces) and two sets of pads worn to 25 and 15 mm. The number of brake pads tested on two brake discs totaled 24. Fig. 22 presents the brake discs. Additionally, thermal images have been recorded of the discs revealing microcracks in the case of the regenerated disc (turned from 110 mm to 108 mm).

During the main investigations, two 610 mm brake discs were tested. In the subsequent tests, a different research program was applied. In the main investigations this was program C with a clamping force of N=28 and 44 kN and a decelerated mass 4.4 and 7.5 t. During the validation tests, research program B was applied from the UIC sheet according to [26]. During the research, for the 590 mm disc, a clamping force of 25 and 36 kN was applied with a decelerated mass of 5.7 t while for the 640 mm disc, a clamping force of 16 and 26 kN and a decelerated mass of 4.7 and 6.7 t was applied.

Figs. 23-25 present the validation of the model of regression according to relation (3) for the results of average coefficient of friction obtained on the test stand.

Then, according to relation (5) the relative percentage error [28] was determined of the fitting of the model of multiple regression of average coefficient of friction to the results of tests on a new 590×110

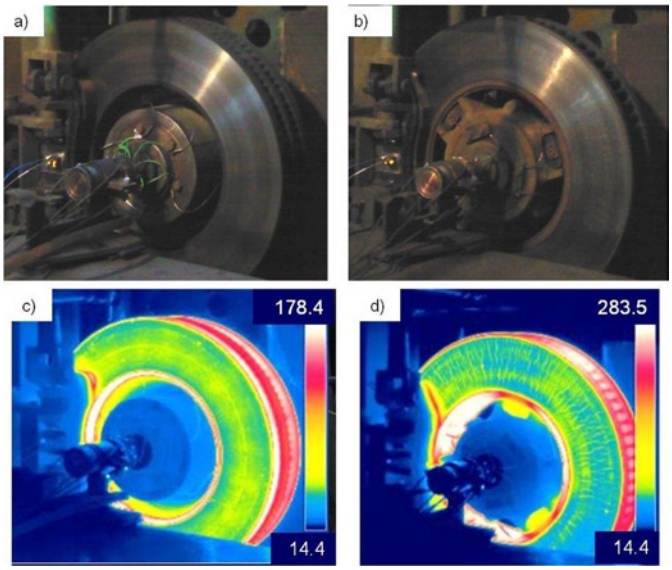

Fig. 22. Object of the investigations on the test stand: a) 590×110 brake disc (new), b) 640×110 brake disc (worn to 108 mm), c) thermal image of a 590×110 brake disc, d) thermal image of the 640×110 brake disc

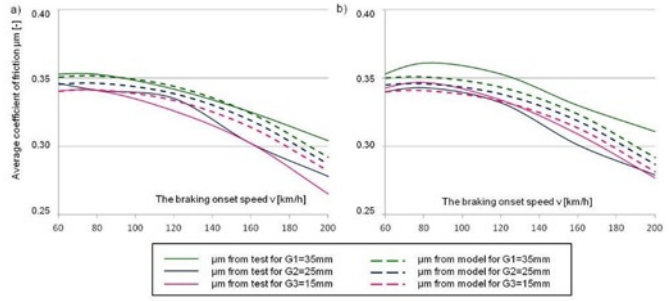

Fig. 23. The relation between μm obtained in the tests and that allowing for the model of multiple regression when braking with a new 590×110 disc with: a) N=25 kN and M=5.7 t, b) N=36 kN and M=5.7 t

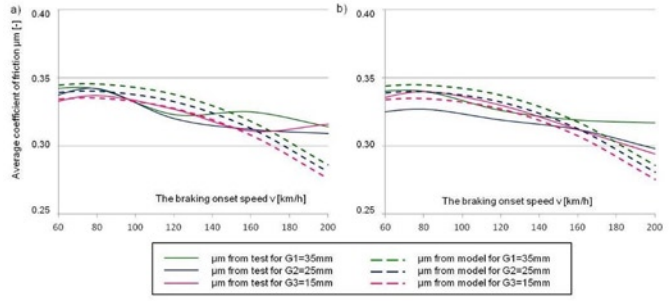

Fig. 24. The relation between μm obtained in the tests and that allowing for the model of multiple regression when braking with a worn 640×110 disc with: a) N=16 kN and M=4.7 t, b) N=26 kN and M=4.7 t

brake disc. Due to the size of the sample $n>30$ (149 brakings) based on inequality (6) the number of classes was ascertained ($k=10$) in order to determine the distribution of the relative percentage error [16]. Based on the relative error data, the maximum x_{max}=13.4 and the minimum value x_{min}=0.03 of the variable was determined, which allowed calculating the data spread of 13.37. Fig 26 presents the percentage of the size of the relative percentage error for 10 classes for the new brake disc.

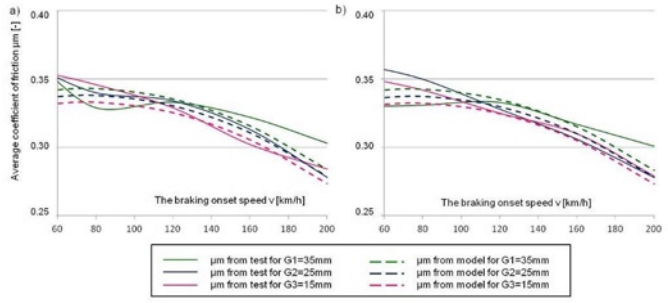

Fig. 25. The relation between μ_m obtained in the tests and that allowing for the model of multiple regression when braking with a worn 640×110 disc with: a) N=28 kN and M=6.7 t, b) N=40 kN and M=6.7 t

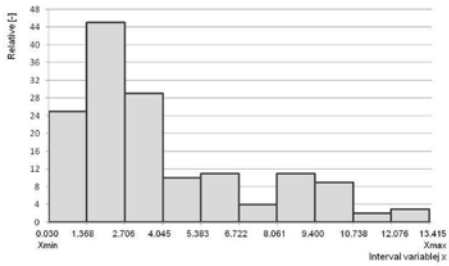

Fig. 26. The histogram of the size of the relative percentage error of the fitting of the model of multiple regression of average coefficient of friction to the results of the tests on a new 590×110 brake disc

Upon the analysis of the histogram presented in Fig. 26, it can be observed that the greatest is the relative percentage error resulting from the non-fitting of the model of multiple regression to the test results in the range of up to 4% that occurred in 60 cases out of 146 observations.

Also, for the regenerated disc, according to relation (5), the relative percentage error [28] was determined of the fitting of the model of multiple regression of the average coefficient of friction (3) to the results of the tests on the 640×110 brake disc. For 237 brakings with different clamping forces and decelerated masses, based on inequality (6) the number of classes was ascertained ($k=11$) in order to determine the distribution of the relative percentage error. Based on the error data, the maximum value x_{max}=14.6 and the minimum value x_{min}=0.05 of the variable were determined, which allowed calculating the data spread of 14.55. Fig. 27 presents the histogram of the size of the relative percentage error for 11 classes for the regenerated brake disc.

Upon analysis of the histogram presented in Fig. 27 it can be observed that the greatest is the relative percentage error resulting from the non-fitting of the model of multiple regression to the test results in the range of up to 7% that occurred in 188 cases out of 237 observations.

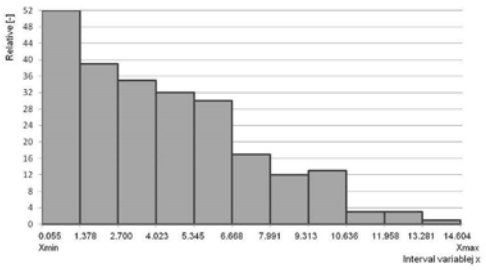

Fig. 27. The histogram of the size of the relative percentage error of the fitting of the model of multiple regression of average coefficient of friction to the results of the tests on a worn 640×110 brake disc

7. Conclusions

The investigations of the friction pair of a disc brake on an approved test stand at Institute of Rail Vehicles 'Tabor' in Poznan have shown that, aside from the preset braking parameters, the coefficient of friction decreases upon wear of both the brake pads and the brake disc below the adopted tolerances according to applicable regulations. The excess of the bottom tolerance of instantaneous and average coefficient of friction already takes place when testing a friction pair of a new brake disc and worn brake pads. This is particularly the case in some braking scenarios i.e. significant clamping forces of the pads on the disc and great decelerated masses. In the extreme cases of the tests, i.e. worn discs and worn brake pads, the reduction of the coefficient of friction is even more conspicuous. It is noteworthy, however, that under actual operation, the wear range is much wider then in the tests. It is to be expected that the values of the coefficient of friction will be even lower for extreme wear of the brake pads (5 mm) and the thickness of the brake disc after regeneration (turning from 110 to 102 mm).

The changes of the coefficient of friction can be modeled to estimate its value by using a series of variable parameters such as the braking onset speed or the decelerated mass. Additionally, it is possible to incorporate the wear of the friction pair components (brake pads and brake disc) in the model of multiple regression. The clamping force on the disc, however, and the decelerated mass have the least significant impact on the changes of the average coefficient of friction.

The tests performed on the test stand on the applied friction pair (organic brake lining and cast iron brake disc) have shown that the requirement of ensuring a constant coefficient of friction in the set ranges was not met. Even though the brake pads made from organic material of an alternative manufacturer were not tested (brake pads currently manufactured and applied in domestic rail vehicles were used) it is justified to include in the brake pad approval regulations a stipulation on the necessity of brake pad testing under an extreme wear scenario in order to validate its variability.

Besides, the results of the tests, based on which the model of changes of the average coefficient of friction was developed, may turn out useful in determining the characteristics of the coefficient of friction depending on the input parameters and wear of the friction pair. Today, when designing vehicle-specific brake calipers, the average value of the coefficient of friction given in sheet UIC 541-3 is introduced, based on which, *inter alia*, the braking distance is calculated. The introduction of a single value μ_m will result in a significant error of the calculated braking distance, where, instead of the imposed value of 0.37, the coefficient of friction assumes values in the range from 0.247 to 0.380.

During the works, the results of which have been presented in the paper, 780 brakings were carried out in order to determine the model of the multiple regression for the average coefficient of friction and 384 brakings to validate the model on subsequent brake discs.

The project has been financed by National Research and Development Centre, project LIDER V, contract number LIDER/022/359/L-5/13/NCBR/2014

References

1. Abbasi S, Teimourimanesh S, Vernersson T, Sellgren U, Olofsson U, Lundén R. Temperature and thermoelastic instability at tread braking using cast iron friction material. Wear 2014; 314: 171-180, https://doi.org/10.1016/j.wear.2013.11.028.
2. Al-Bender F, Lampaert V, Swevers J. The generalized Maxwell-Slip Model: A novel model for friction simulation and compensation. IEEE Transactions on Automatic Control 2005; 50(11): 1883-1887, https://doi.org/10.1109/TAC.2005.858676.
3. Aranganathan N, Jayashree B. Development of copper-free eco-friendly brake-friction material using novel ingredients. Wear 2016; 352-353: 79-91, https://doi.org/10.1016/j.wear.2016.01.023.
4. Awrejcewicz J, Grzelczyk D, Pyryev Y. A novel friction modeling and its impact on differential equations computation and Lyapunov exponents estimation, Vibromechanika. Journal of Vibroengineering 2008; 10(4): 475-482.
5. Bagnoli F, Dolce F, Bernabei M. Thermal fatigue cracks of fire fighting vehicles gray iron brake disc. Engineering Failure Analysis 2009; 16: 152-163, https://doi.org/10.1016/j.engfailanal.2008.01.009.
6. Baranowski P, Damaziak K, Małachowski J. Brake system studies using numerical methods. Eksploatacja i Niezawodnosc – Maintenance and Reliability 2013; 15(4): 337–342.
7. Baranowski P, Damaziak K, Małachowski J Sergienko V.P. Bukharov S N. Modeling of Abrasive Wear by the Meshless Smoothed Particle Hydrodynamics Method. Journal of Friction and Wear 2016; 37(1): 94–99, https://doi.org/10.3103/S1068366616010037.
8. Basic ADAMS Full Simulation Training Guide, http://support.mscsoftware.com
9. Belhocine A, Bouchetara M. Thermomechanical modelling of dry contacts in automotive disc brake. International Journal of Thermal Sciences 2012; 60: 161-170, https://doi.org/10.1016/j.ijthermalsci.2012.05.006.
10. Betancourt S J, Cruz A. Friction and wear in sliding contact of cast iron against phenolic resin composites reinforced with carbonaceous fibres from plantain fibre bundles. Lubrication Science 2013; 25: 163-172, https://doi.org/10.1002/ls.1186.
11. Chichinadze A V. Theoretical and practical problems of thermal dynamics and simulation of the friction and wear of tribocouples. Journal of Friction and Wear 2009; 30: 199–215, https://doi.org/10.3103/S106836660903009X.
12. Canadus de Wit C, Olson H, Åström K J, Lischinsky P. A new model for control of systems with friction. IEEE Transactions on Automatic Control 1995; 40(3): 419-425, https://doi.org/10.1109/9.376053.
13. Collignon M, Regheere G, Cristol A.L, Desplanques Y, Balloy D. Braking performance and influence of microstructure of advanced cast irons for heavy goods vehicle brake discs. Journal of Engineering Tribology 2013; 227(8): 930-940, https://doi.org/10.1177/1350650113484212.
14. Crăciun A. Evolution of materials for motor vehicles brake discs, ANNALS of Faculty Engineering Hunedoara. International Jurnal of Engineering 2015; 13(3): 149-154.
15. Dokumentacja Systemu Utrzymania – czteroosiowy piętrowy wagon pasażerski 2 klasy typu DBme serii Bmnopux nr DSU-DBme 0130-1. Przewozy Regionalne spółka z o. o. Warszawa 2010; 12: 70-76.
16. Gajek L, Kałuszka M. Wnioskowanie statystyczne – modele i metody. WNT, Warszawa 2000: 90-95.
17. Głowacz A, Głowacz W, Glowacz Z, Kozik J. Early fault diagnosis of bearing and stator faults of the single-phase induction motor using acoustic signals, Measurement 2018; 113: 1-9, https://doi.org/10.1016/j.measurement.2017.08.036.

18. Głowacz A, Głowacz Z. Diagnosis of stator faults of the single-phase induction motor using acoustic signals. Applied Acoustics Part A 2017; 117: 20-27, https://doi.org/10.1016/j.apacoust.2016.10.012.
19. Gruszewski M. Wybrane zagadnienia eksploatacji hamulca tarczowego. Technika transport szynowego 1995; 6-7: 84-86.
20. Grzes P, Oliferuk W, Adamowicz A, Kochanowski K, Wasilewski P, Yevtushenko A.A. The numerical-experimental scheme for the analysis of temperature field in a pad-disc braking system of a railway vehicle at single braking. International Communications in Heat and Mass Transfer 2016; 75: 1-6, https://doi.org/10.1016/j.icheatmasstransfer.2016.03.017.
21. Kikuuwe R, Takesue N, Sano A, Mochiyama H, Fujimoto H. Fixed-step friction somulation: from classical Coulomb model to modern continuous models. Proceedings of IEEE/RSJ International Conference on Intelligent Robots and Systems 2005: 3910-3917.
22. Kamiński Z, Kulikowski K. Determination of the functional and service characteristics of the pneumatic system of an agricultural tractor with mechanical brakes using simulation methods. Eksploatacja i Niezawodnosc – Maintenance and Reliability 2015; 17(3): 355–364, https://doi.org/10.17531/ein.2015.3.5.
23. Kasem H, Brunel J.F, Dufrénoy P, Siroux M, Desmet B. Thermal levels and subsurface damage induced by the occurrence of hot spots during high-energy braking. Wear 2011; 270: 355-364, https://doi.org/10.1016/j.wear.2010.11.007.
24. Kinkaid N.M, O'Reilly O.M, Papadopoulos P. Automotive disc brake squeal. Journal of sound and vibration 2003; 267: 105-166. https://doi.org/10.1016/S0022-460X(02)01573-0
25. KNORR-BREMSE Brake Disc and Pads. Application freight cars, high-speed train, light rail vehicles, locomotives, metros, passenger coaches, regional and commuter trains. P-1264-EN. 2014; 9:1-4.
26. Kodeks UIC 541–3. Hamulec–Hamulec tarczowy i jego zastosowanie. Warunki dopuszczenia okładzin hamulcowych. Wydanie 7, czerwiec 2010: 10-24.
27. KOMISJA Decyzja komisji z dnia 28 lipca 2006 r. dotycząca technicznej specyfikacji dla interoperacyjności odnoszącej się do podsystemu tabor kolejowy – wagony towarowe transeuropejskiego systemu kolei konwencjonalnych 2006/861/WE, Załącznik I, podpunkt I.9: 242-243.
28. Krysicki W, Włodarski L. Analiza matematyczna w zadaniach, Wydawnictwo PWN, Warszawa 2007: 412-426.
29. Kumar M, Boidin X, Desplanques Y, Bijwe J. Influence of various metallic fillers in friction materials on hot-spot appearance during stop braking. Wear 2011; 270: 371-381, https://doi.org/10.1016/j.wear.2010.11.009.
30. Lampaert V, Swevers J, Al-Bender F. Modyfication of the Leuven integrated friction model structure. IEEE Transactions on Automatic Control 2002; 47(4): 683-687, https://doi.org/10.1109/9.995050.
31. Lang A.M, Smales H. An approach to the solution of disc brake vibration problems, in: Braking of Road Vehicles. Automobile Division of the Institution of Mechanical Engineers, Mechanical Engineering Publications Limited, Suffolk, England 1993: 223-231.
32. Leszek W. Wybrane zagadnienia metodyczne badań empirycznych. Instytut Technologii Eksploatacji, Radom 2006: 142-153.
33. Li Z, Han J, Yang Z, Li W. Analyzing the mechanisms of thermal fatigue and phase change of steel used in brake discs. Engineering Failure Analysis 2015; 57: 202-218, https://doi.org/10.1016/j.engfailanal.2015.07.002.
34. Liang J, Fillmore S, Ma O. An extended bristle friction force model with experimental validation. Mechanism and Machine Theory 2012; 56, 2012: 123-137.
35. Mańczak K. Technika planowania eksperymentu, Wydawnictwo Naukowo-Techniczne, Warszawa 1976: 76-84.
36. Meierhofer A, Hardwick C, Lewis R, Six K, Dietmaier P. Third body layer-expermental results and a model describing its influence on the traction coefficient. Wear 2014; 314: 148-154, https://doi.org/10.1016/j.wear.2013.11.040.
37. Müller M, Ostermeyer G.P. A cellular automaton model to describe the three dimensional friction and wear mechanism of brake systems. Wear 2007; 263: 1175–1188, https://doi.org/10.1016/j.wear.2006.12.022.
38. Nosal S, Orłowski T. Wpływ wybranych napełniaczy na właściwości ciernych materiałów hamulcowych. Tribologia 2009; 2: 119-126.
39. Nosal S, Orłowski T. Wpływ rodzaju użytego grafitu I koksu naftowego na właściwości tarciowo-zużyciowe materiałów ciernych. Tribologia 2010; 2: 85-93.
40. Padthe A. K, Oh J, Bernstein D S. On the LuGre model and friction-induced hysteresis. Proceedings of the 2006 American Control Conference, Minneapolis, Minnesota, USA 2006: 3247-3252, https://doi.org/10.1109/ACC.2006.1657218.
41. Panier S, Dufrénoy P, Weichert D. An experimental investigation of hot spots in railway disc brakes. Wear 2004; 256: 764-773, https://doi.org/10.1016/S0043-1648(03)00459-9.
42. Peveca M, Oder G, Potrč I, Šraml M. Elevated temperature low cycle fatigue of grey cast iron used for automotive brake discs. Engineering Failure Analysis, 2014; 42: 221-230, https://doi.org/10.1016/j.engfailanal.2014.03.021.
43. Polska Norma PN-EN 14531-1, Kolejnictwo – Metody obliczania dróg hamowania do zatrzymania lub do określonej prędkości oraz metody obliczania hamulca postojowego – Część 1: Algorytmy ogólne z zastosowaniem średniej wartości obliczeniowej dla pociągów lub pojedynczych pojazdów. Warszawa luty 2016: 11-19.
44. Polska Norma PN-EN 14535-1, Kolejnictwo – tarcze hamulcowe kolejowych pojazdów szynowych – Część 1: Tarcze hamulcowe wtłaczane lub mocowane skurczowo na osiach zestawów tocznych lub napędnych, wymiary i wymagania dotyczące jakości, Warszawa 2006: 22-23.
45. Polska Norma PN-EN 14535-3 Kolejnictwo – Tarcze hamulcowe kolejowych pojazdów szynowych – Część 3: Tarcze hamulcowe, właściwości tarczy i pary ciernej, klasyfikacja. Warszawa luty 2016: 12-16.
46. Rail Consult Gesellschaft für Verkehrsberatung mbH, Wagon osobowy Z1 02 – układ jezdny–tom2. Dokumentacja Techniczno-Ruchowa: 46-59.
47. Rozporządzenie Komisji (UE) NR 321/2013 z dnia 13 marca 2013 r. dotyczące technicznej specyfikacji interoperacyjności odnoszącej się do podsystemu Tabor- wagony towarowe systemu kolei w Unii Europejskiej i uchylające decyzję 2006/861/WE: 17-18.
48. Rozporządzenie Komisji (UE) NR 1302/2014 z dnia 18 listopada 2014 r. w sprawie technicznej specyfikacji interoperacyjności odnoszącej się do podsystemu Tabor – lokomotywy i tabor pasażerski systemu kolei w Unii Europejskiej, Dodatek J Nr indeksu 24: 272-274, 388-389.
49. Saumweber E. Auslegung und Leistungsgrenzen von Scheibenbremsen. ZEV-Glasses Annalen 1988; 112(4): 139-143.
50. Szymanski G M, Josko M, Tomaszewski F, Filipiak R. Application of time-frequency analysis to the evaluation of the condition of car suspension. Mechanical System and Signal Processing 2015; 58-59: 298-308, https://doi.org/10.1016/j.ymssp.2014.12.017.
51. Szymanski G M, Josko M, Tomaszewski F. Diagnostics of automatic compensators of valve clearance in combustion engine with the use of vibration signal. Mechanical System and Signal Processing 2016; 68-69: 479-490, https://doi.org/10.1016/j.ymssp.2015.07.015.

52. Ścieszka S.F. Hamulce cierne. Zagadnienia materiałowe, konstrukcyjne i tribologiczne. Wydawnictwo Gliwice-Radom 1998: 11-19.
53. UNITED NATIONS Regulation No. 90, Addendum 89: Uniform provisions concerning the approval of replacement brake lining assemblies, drum brake linings and discs and drums for power-driven vehicles and their trailers. E/ECE/324/Rev.1/Add.89/Rev.3-E/ECE/TRANS/505/Rev.1/Add.89/Rev.3, 17 February 2012: 17-21.
54. Webside http://breck.pl/pl/produkty/klocki-breck-hs/
55. Wojewoda J, Stefański A, Wiercigroch M, Kapitaniak T. Hysteretic effects in dry friction: modelling and experimental studies. Philosophical Transactions of the Royal Society A 2008: 366: 753-757, https://doi.org/10.1098/rsta.2007.2125.
56. Wu S C, Zhang S Q, Xu Z W. Thermal crack growth-based fatigue life prediction due to braking for a high-speed railway brake disc. International Journal of Fatigue. 2016; 87: 359-369, https://doi.org/10.1016/j.ijfatigue.2016.02.024.
57. Wirth X., Improving the Performance of Disc Brakes on High-speed Rail Vehicles with a Novel Types of Brake Pad: Isobar. RTR 1998; 1: 24-29.

Wojciech SAWCZUK
Institute of Combustion Engines and Transport
Poznan University of Technology
ul. Piotrowo, 60-965 Poznań, Polska

E-mail: wojciech.sawczuk@put.poznan.pl